Electronic Supplementary Material (ESI) for Chemical Communications

Electronic Supplementary Information

Thermally/hydrolytically Stable Covalent Organic Frameworks from a Rigid Macrocyclic Host

Jing-Ru Song,[a] Junliang Sun,[*b] Junmin Liu,[*c] Zhi-Tang Huang[a] and Qi-Yu Zheng[*a]

[a] Beijing National Laboratory for Molecular Sciences, CAS Key Laboratory of Molecular Recognition and Function, Institute of Chemistry, Chinese Academy of Sciences, Beijing, 100190, China.

[b] Beijing National Laboratory for Molecular Sciences, College of Chemistry and Molecular Engineering, Peking University, Beijing, 100871, China.

[c] Klghei of Environment and Energy Chemistry, School of Chemistry and Chemical Engineering, Sun Yat-Sen University, Guangzhou, 510275, China.

Experimental section

1. Materials and measurement

IR spectra were recorded on a Thermo-Nicolet 6700 spectrometer using KBr discs. ^{13}C CP-MAS NMR spectra data were collected on a BRUKER AVANCE III 400MHz solid state NMR spectrometer. Element analysis for C, H and N were carried out with a Flash EA 1112 elemental analyzer. Thermogravimetric analysis was performed on SDT Q600 V20.9 Build 20 with a temperature ramping rate of 10 ^{o}C min^{-1} from room temperature to 900 ^{o}C. Scanning electron microscopy (SEM) was performed on S-4300 scanning electron microscope at 15.0 KV. Powder X-ray diffraction (PXRD) data were recorded on a Rigaku D/max 2500 X-ray powder diffractometer, from 2θ =2^{o} up to 50^{o} with 0.02^{o} increment. Nitrogen adsorption– desorption isotherms were carried out with a Micrometrics ASAP 2020 instrument at 77 K , hydrogen adsorption isotherms were measured at 77 K from 0 to 823 mmHg on Micrometric ASAP 2020 instrument. Carbon dioxide adsorption isotherms were measured at 298 K from 0 to 50 bar on Belsorp-HP. CD spectra was performed on J-815 using KBr discs. Geometry optimization of the hexagonal pore structure was performed at Forcite Module in Material Studio 6.0. CTV-CHO was synthesized according to the literature[1]. All chemicals were used as received without further purification unless stated otherwise.

2. Synthesis

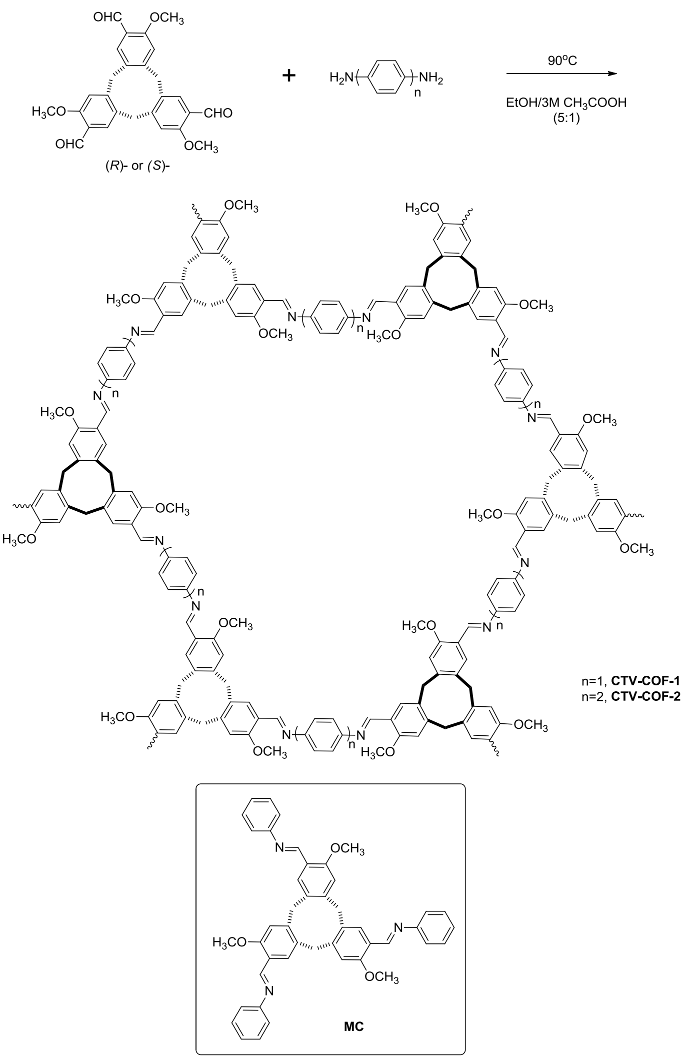

Model Compound (MC): A 25 ml flask was charged with triformylcyclotrianisylene (CTV-CHO) (59 mg, 0.13 mmol), 10 ml dry EtOH was added and heated to reflux under nitrogen. Aniline (74.3 mg, 0.80 mmol) was added by syringe. The mixture was reacted overnight. After cooled to room temperature, reduced the solvent in vacuum to about 2 ml, yellow powder was obtained after filtration. Washed the powder with cold EtOH, then dried in vacuum, 75 mg white solid product was obtained with 84% yield. Mp > 300^{o}C; FTIR *v* 2933, 1678, 1620, 1604, 1585, 1483, 1405, 1267, 1199, 1020, 768, 723, 693 cm^{-1}; ^{1}HNMR (400MHz, $CDCl_3$) δ 8.767 (s, 3H), 8.194 (s, 3H), 7.367 (t, 6H, J=7.6Hz), 7.218-7.153 (m, 9H), 7.064 (s, 3H), 4.809 (d, 3H, J=13.2Hz), 3.896-3.827 (m, 12H); ^{13}CNMR (400MHz, $CDCl_3$) δ 158.541, 156.216, 153.0, 144.947, 131.156, 129.135, 128.792, 125.652, 123.549, 121.123, 112.690, 55.874, 36.614; HRMS (ESI) 670.30729 ($[M+H]^+$).

CTV-COF-1: A 25 ml Schlenk tube was charged with CTV-CHO (100 mg, 0.225 mmol), 1,4-benzenediamine (37 mg, 0.34 mmol) and 6.0 ml of a 5:1 (v/v) solution of EtOH/3M CH_3COOH. The tube was evacuated to vacuum (-0.095MPa) at 77 K (LN_2 bath) and then sealed. The reaction mixture was heated at 90 ^{o}C for 5 days. The product was isolated by filtration, washed with acetone, and then soaked in HPLC acetone for 8h. After filtration, the powder was dried under vacuum at 120 ^{o}C for 12h. 113 mg yellow powder was obtained with 91% yield. FTIR *v* 2932, 1682, 1624, 1601, 1494, 1463, 1266, 1200, 1176, 1084, 835 cm^{-1}; ^{13}C CP-MAS NMR (400 MHz, solid state) δ 156.79, 148.87, 144.00, 130.61, 122.44, 116.14, 110.19, 52.64, 36.46; Anal. calcd. for $(C_{12}H_{10}NO)_n$, C 78.26, H 5.43, N 7.60, Found: C 76.15, H 5.72, N 7.44.

CTV-COF-2: The procedure is similar to above: CTV-CHO (100 mg, 0.225 mmol), benzidine (62 mg, 0.337 mmol) and 6.0 ml solution of EtOH/3M CH_3COOH. Yellow power was obtained in 94% yield. FTIR *v* 2922, 1681, 1620, 1606, 1487, 1463, 1403, 1269, 1202, 1167, 1083, 1016, 825 cm^{-1}; ^{13}C CP-MAS NMR (400 MHz, solid state) δ 156.81, 148.87, 144.08, 136.34, 130.32, 125.81, 122.42, 110.45, 52.80, 36.32; Anal. calcd. for $(C_{16}H_{12}NO)_n$, C 82.05, H 5.13, N 5.98, Found: C 78.24, H 5.48, N 6.09.

Electronic Supplementary Material (ESI) for Chemical Communications

3. NMR spectra for MC

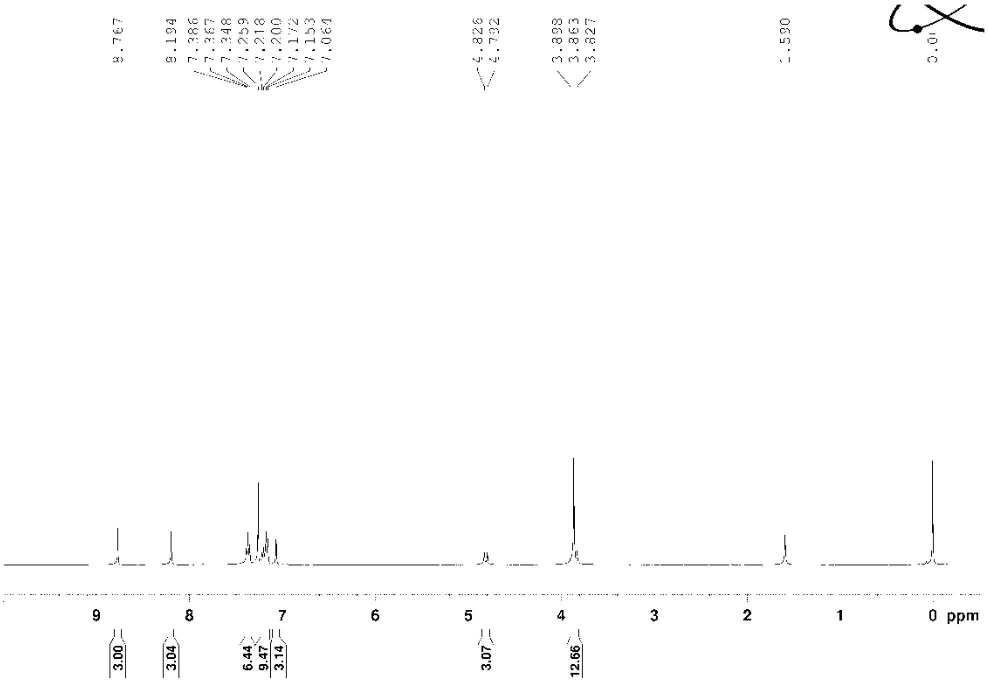

Fig. S1 ^{1}HNMR for Model Compound (MC).

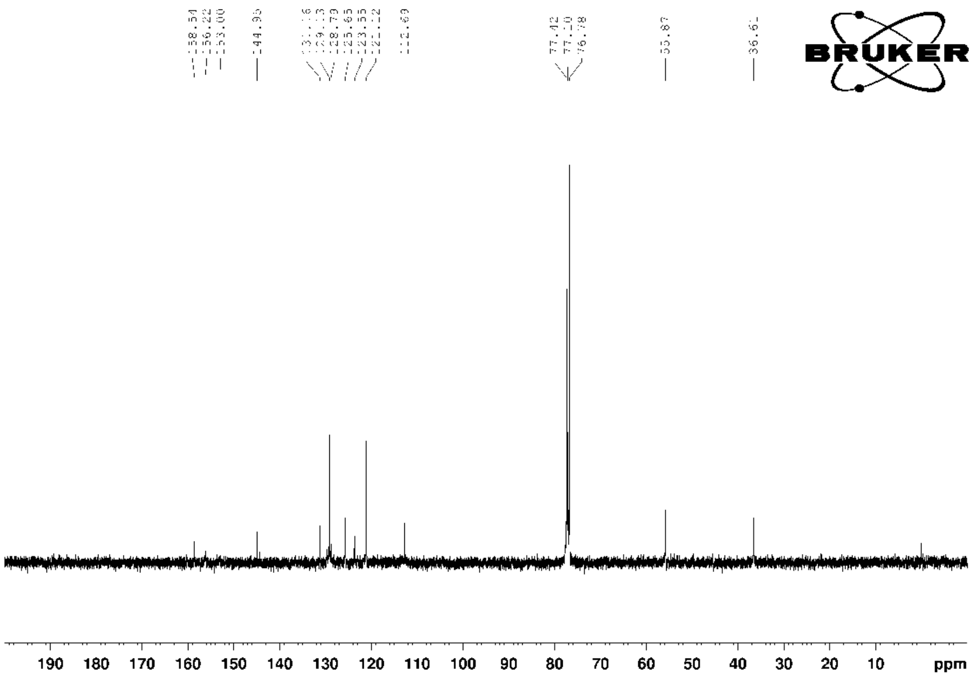

Fig. S2 ^{13}CNMR for Model Compound (MC).

Electronic Supplementary Material (ESI) for Chemical Communications

4. FTIR spectra

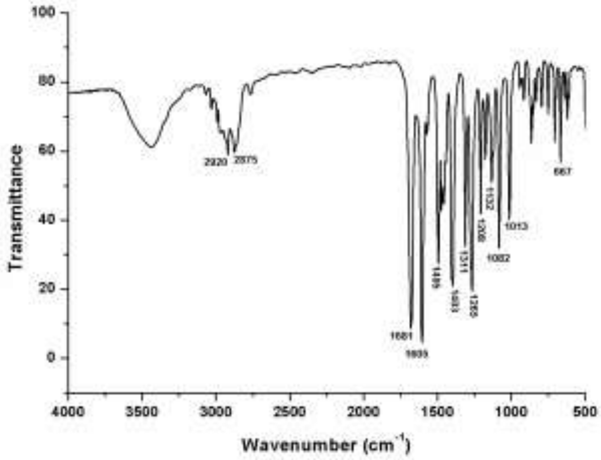

Fig. S3 The FTIR spectra of CTV-CHO.

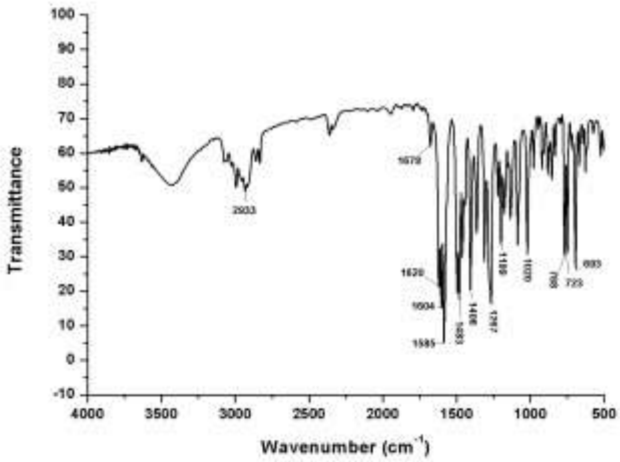

Fig. S4 The FTIR spectra for MC.

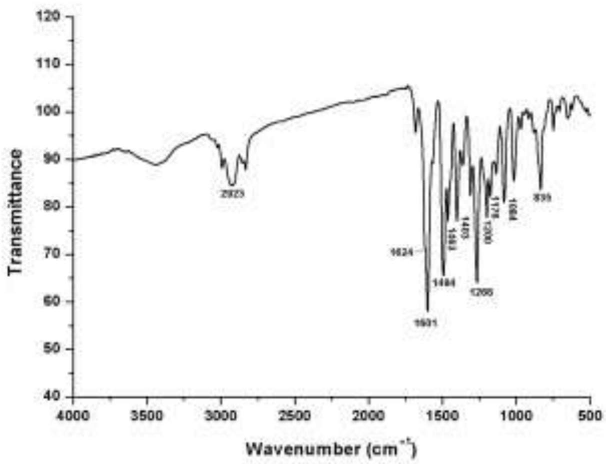

Fig. S5 The FTIR spectra of CTV-COF-1.

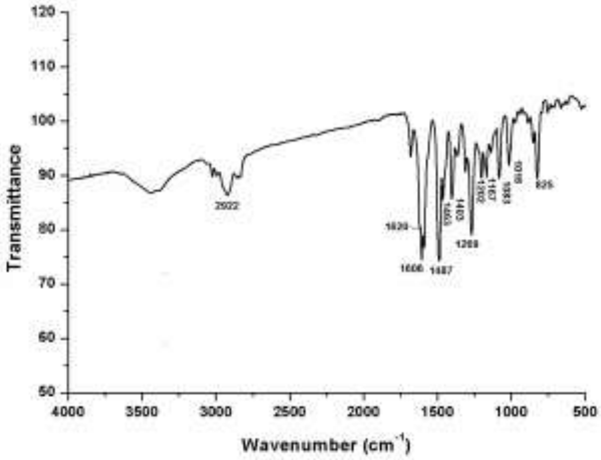

Fig. S6 The FTIR spectra of CTV-COF-2.

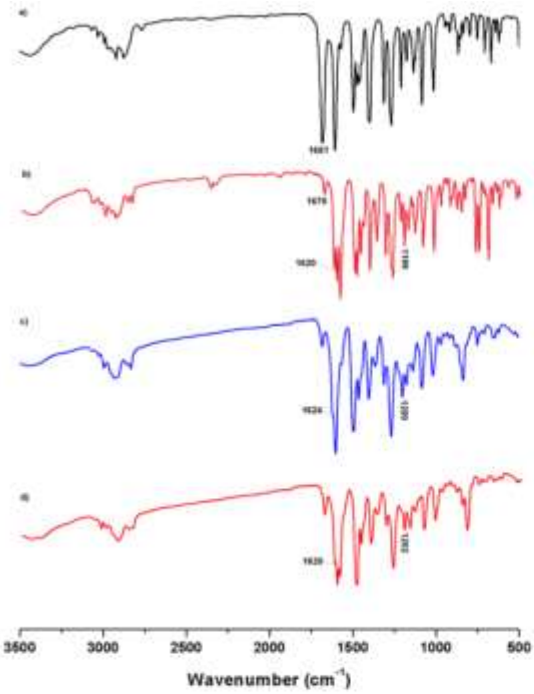

Fig. S7 The FTIR spectra for a) CTV-CHO (black); b) MC (pink); c) CTV-COF-1 (blue); d) CTV-COF-2 (red).

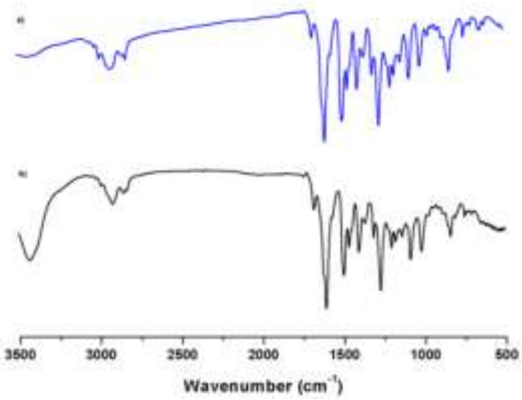

Fig. S8 The FTIR spectra for a) CTV-COF-1; b) CTV-COF-1 in water for 48h.

5. ^{13}C CP-MAS NMR spectra for CTV-COFs

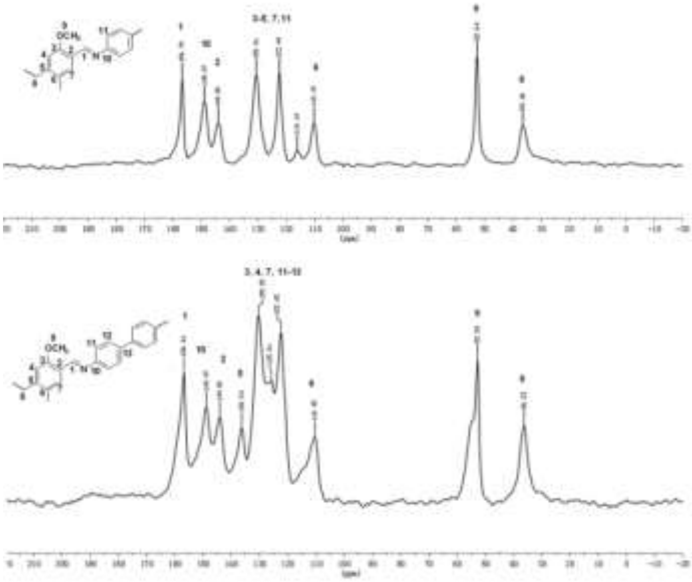

Fig. S9 ^{13}C CP-MAS NMR spectra for CTV-COFs.

6. TGA measurement for CTV-COFs

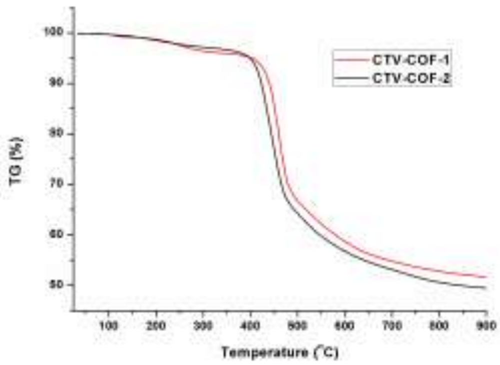

Fig. S10 TGA measurement for CTV-COF-1 (red) and CTV-COF-2 (black).

7. SEM images for CTV-COFs

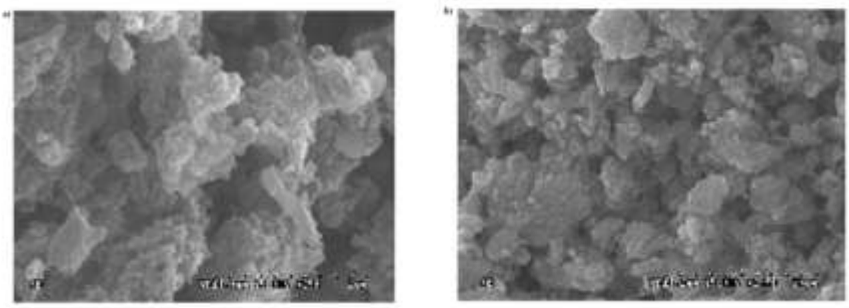

Fig. S11 SEM spectra for a) CTV-COF-1; b) CTV-COF-2.

8. PXRD

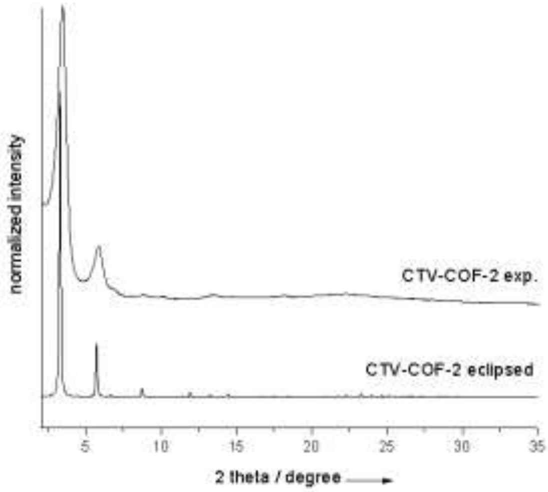

Fig. S12 Comparison of the experimentally observed PXRD pattern with the simulated eclipsed pattern for CTV-COF-2.

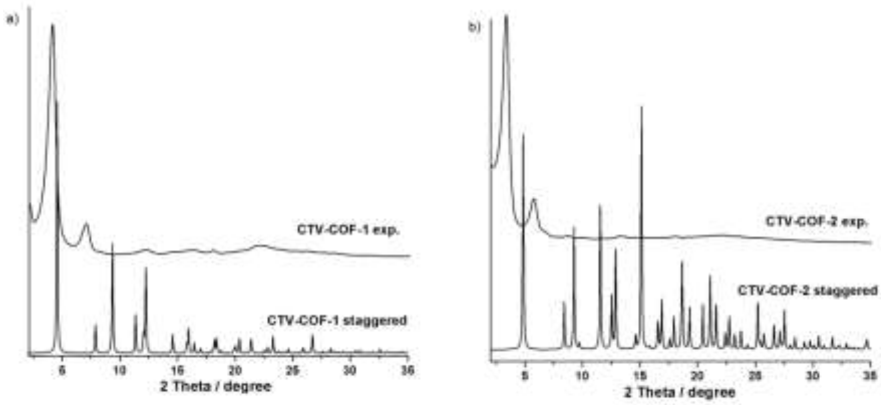

Fig. S13 Comparison of the experimentally observed PXRD pattern with the simulated staggered pattern. a) CTV-COF-1, b) CTV-COF-2.

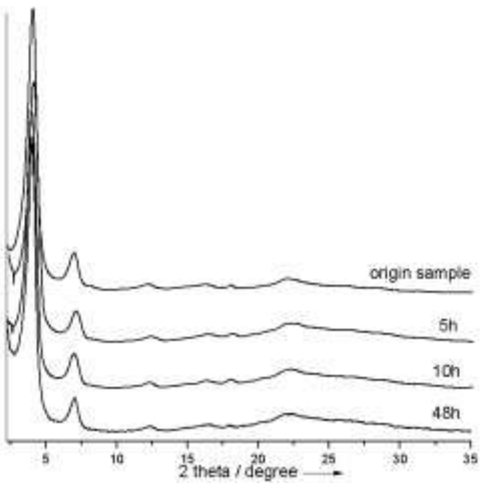

Fig. S14 PXRD patterns for the hydrolytic test of CTV-COF-1.

9. N_2 uptake

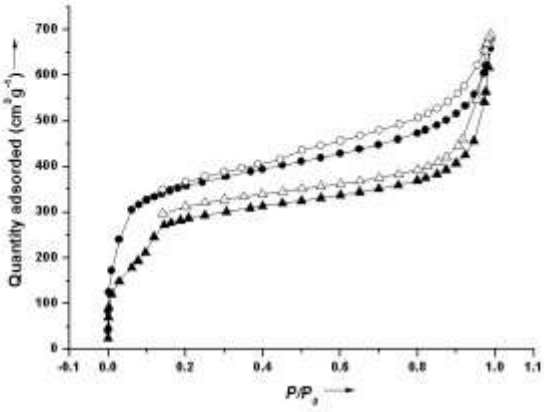

Fig. S15 Nitrogen sorption isotherms (filled simples for adsorption and open simples for desorption). Cycle for CTV-COF-1 and triangle for CTV-COF-2

10. BET plot and pore size distribution for CTV-COFs

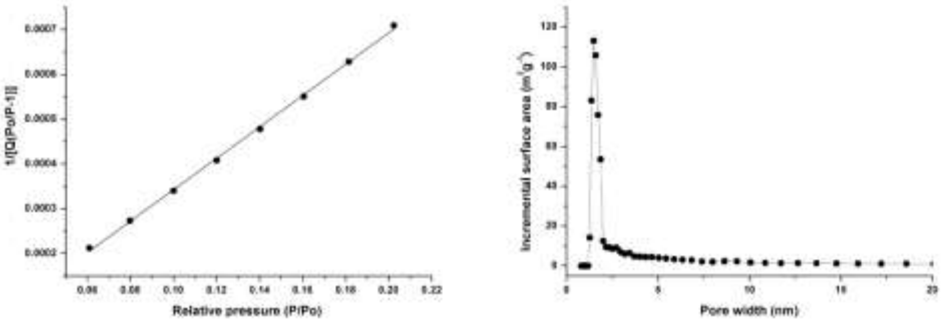

Fig. S16 BET plot and pore size distribution of CTV-COF-1.

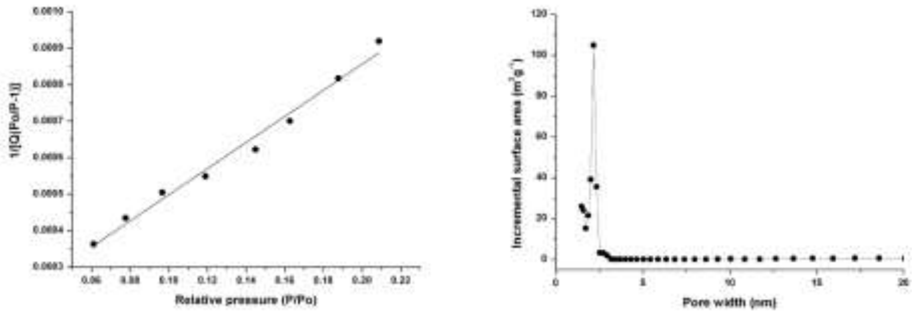

Fig. S17 BET plot and pore size distribution of CTV-COF-2.

11. Models of CTV-COFs

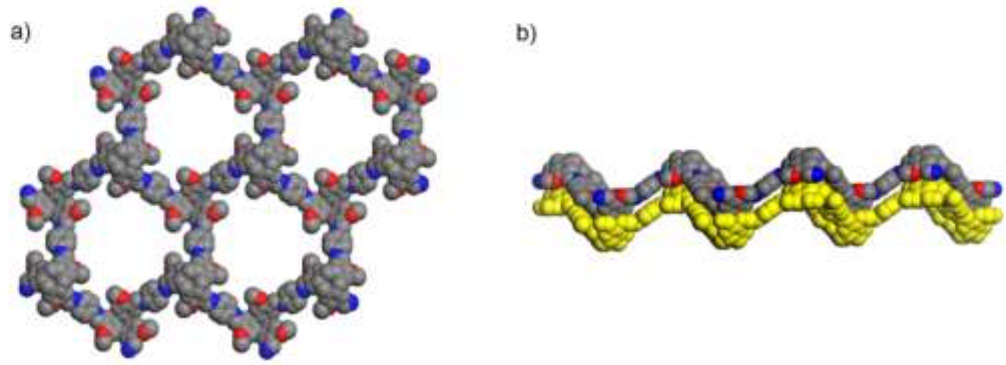

Fig. S18 Top view (a) and side view (b) of eclipsed CTV-COF-1. C gray, O red, N blue. All hydrogen atoms are omitted for clarity, adjacent layers are coloured in yellow.

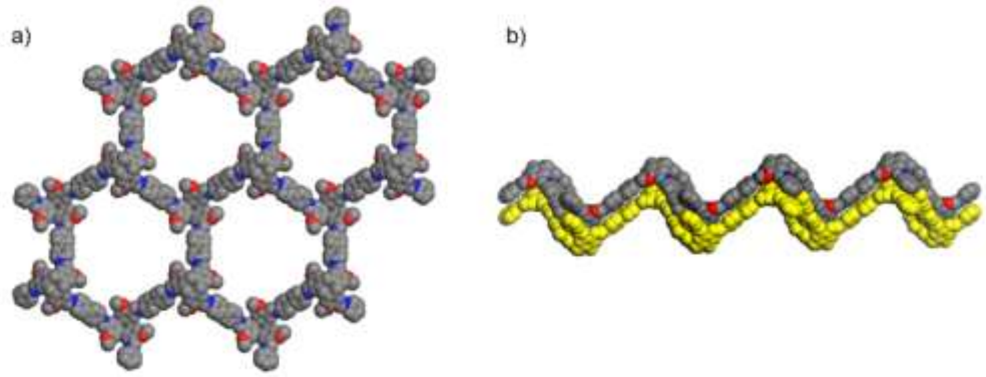

Fig. S19 Top view (a) and side view (b) of eclipsed CTV-COF-2. C gray, O red, N blue. All hydrogen atoms are omitted for clarity, adjacent layers are coloured in yellow.

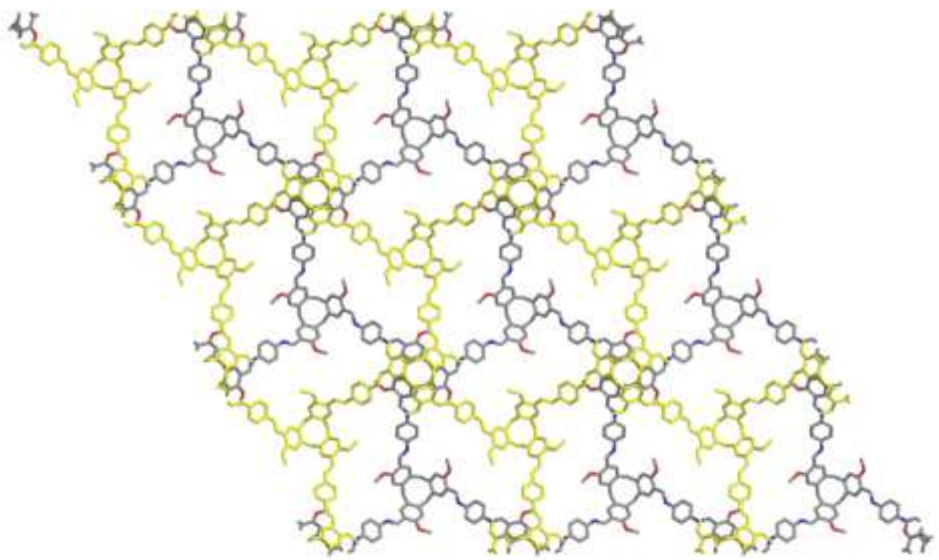

Fig. S20 Top view staggered CTV-COF-1. C gray, O red, N blue. All hydrogen atoms are omitted for clarity, another layer is coloured in yellow.

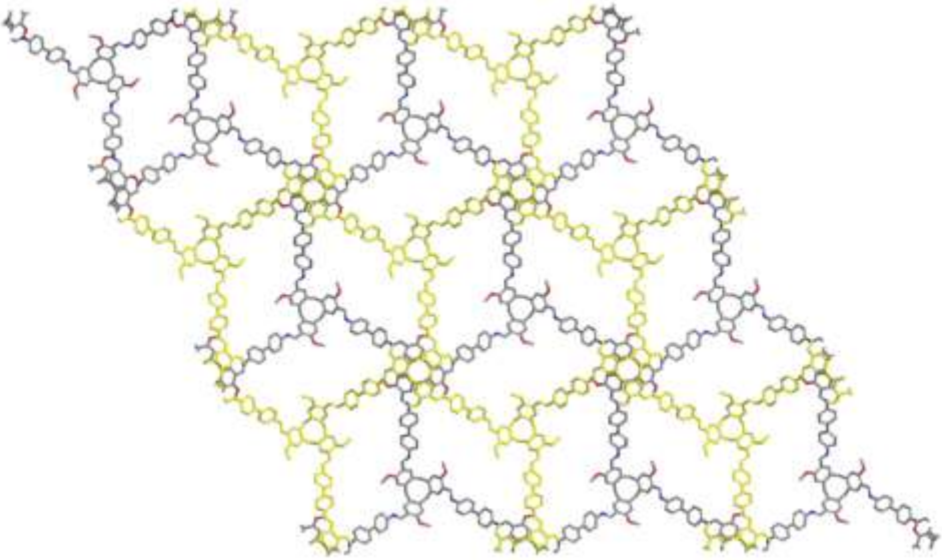

Fig. S21 Top view staggered CTV-COF-2. C gray, O red, N blue. All hydrogen atoms are omitted for clarity, another layer is coloured in yellow.

12. CD spectra

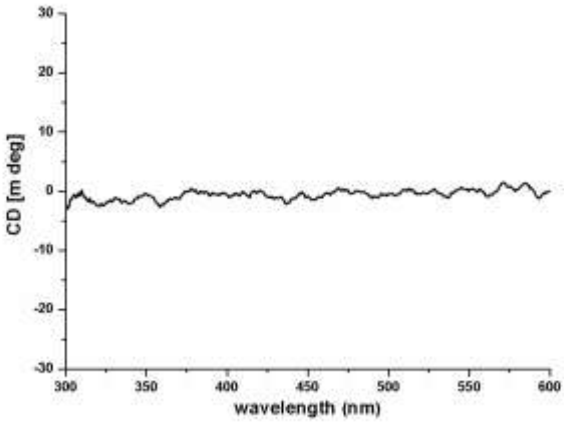

Fig. S22 CD spectra of CTV-COF-2.

13. Tables

Table S1. Comparison of CTV-COF-1-xh.

COFs	S_{BET}[a] / m^2g^{-1}	S_{micro}[b] / m^2g^{-1}	V_{total}[c] / cm^3g^{-1}	V_{micro}[d] / cm^3g^{-1}
CTV-COF-1	1245	573	0.9345	0.2582
CTV-COF-1-5h	1127	563	0.8729	0.2524
CTV-COF-1-10h	1085	555	0.8675	0.2445
CTV-COF-1-48h	997	505	0.7655	0.2236

Table S2. Fractional atomic coordinates for the unit cell of CTV-COF-1.

CTV-COF-1			
a=*b*=22.9544, *c*=4.5691 space volume=2084.94			
atom	x	y	z
C1	0.47615	0.21793	-0.71845
C2	0.51885	0.20690	-0.90404
C3	0.57028	0.25948	-1.06699
C4	0.57749	0.32437	-1.05523
C5	0.53536	0.33515	-0.86853
C6	0.48537	0.28316	-0.69926
C7	0.44510	0.29820	-0.49146
C8	0.36913	0.34348	-0.10457
C9	0.47436	0.44923	-0.10580
C10	0.43509	0.38358	-0.21077
H1	0.51325	0.15743	-0.92116
H2	0.54180	0.38506	-0.85504
H3	0.40329	0.25736	-0.37800
H4	0.52514	0.48065	-0.18606
H5	0.33701	0.29296	-0.18478
N	0.46460	0.36024	-0.42381

Table S3. Fractional atomic coordinates for the unit cell of CTV-COF-2.

CTV-COF-2			
a=*b*=30.8566, *c*=4.4576 space volume=3675.6			
atom	x	y	z
C1	0.43404	0.45707	2.46585
C2	0.38756	0.42716	2.60836
C3	0.36675	0.44847	2.79387
C4	0.39183	0.50041	2.84084
C5	0.43778	0.53042	2.69951
C6	0.45836	0.50927	2.51076
C7	0.32609	0.50582	3.11088
C8	0.31114	0.53472	3.30781
C9	0.26093	0.52316	3.31954
C10	0.24836	0.55266	3.50148
C11	0.28474	0.59319	3.66887
C12	0.33499	0.60382	3.66139
C13	0.34734	0.57453	3.47896
N	0.52387	0.37271	1.70350
H1	0.38577	0.58275	3.47195

H2	0.21012	0.54471	3.51362
H3	0.33199	0.42395	2.90766
H4	0.36782	0.38686	2.58847
H5	0.45744	0.57057	2.73292
H6	0.49307	0.53425	2.39807
H7	0.29741	0.47116	3.01328

References

(1) D. Xu and R. Warmuth, *J. Am. Chem. Soc*., 2008, **130,** 7520.